The effect of some physical and geometrical parameters on improvement of the impact response of smart composite structures

F. Ashenai Ghasemi, A. Shokuhfar, S. M. R. Khalili, G. H. Payganeh and K. Malekzadeh

***Abstract*—** This article presents a complete analytical model to study the role of the shape memory alloys (SMAs) on improvement the impact response of the smart composite structures. The role of some physical and geometrical parameters such as the volume fraction, the orientation and the location of the SMA wires on the contact force history, the deflection, the in-plane strains and stresses of the structures is investigated in details. Also the effect of density of the impactor to the plate ratio and the elastic modulus of the impactor to the plate ratio on the contact force history and the deflection of the plate is studied. The first order shear deformation theory as well as the Fourier series method was utilized to solve the governing equations of the composite plate analytically. The interaction between the impactor and the plate was modeled with the help of two degrees of freedom system consisting of springs-masses. The Choi's linearized contact model was used in the analysis. The results of the above research indicated that the use of the SMA wires inside the smart composite structures improve the global behavior of the structure against the impact. The smart composite structures damp more uniformly and rapidly after the impact.

***Keywords*—** impact, smart composite, SMA wires, springs-masses model.

I. Introduction

Recently, many attentions have been attracted to the polymer based composite structures [1], [2]. The greatest advantage of them is their high stiffness and strength combined with lightness. Currently the interest in use of shape memory alloy (SMA) wires in the traditional composite structures is increased. Shape memory composite structures have the capacity to recover large strains imposed by mechanical loadings, heating cycles or an electric field. Such materials serves as key components in intelligent or smart structures, since they can respond (change shape/stiffness) in the present of external stimulus. Embedding the SMA wires inside the traditional polymer composites can reinforce the damage tolerance of multilayered composite structures. This is because the excited SMA wires can generate recovery tensile stresses inside the structure and hence reduce the deflection and the in plane strains and stresses in transverse loadings. The effect of low velocity impact on the composite structures and prestressing of these structures was extensively studied in the past by Abrate [3], Olsson [4] - [5], and Sun *et al.* [6] and many others. Birman *et al.* [7] demonstrated that if the SMA wires are embedded within the traditional polymer composite plates, tensile stresses that results in heating of the wires, increases the impact resistance of the structure. He also showed that the SMA wires would decrease global deflection of the structure. He used constitutive relationship and associated micro-mechanics, which were considered in a number of studies (Zhong *et al.* [8], and Rogers [9]). In addition, some of the researchers (Rogers [9], and Schetky [10]) verified the above theories by experiments. Roh *et al.* [11] embedded the SMA wires inside a traditional multilayered laminated composite structure and utilized the energy balance and the FEM method to study the effect of the same parameters worked by Birman *et al.* [7].

The objective of this article is to develop a complete model using the simultaneous analytical applications of the Choi's linearized contact law, the springs-masses model, and the Fourier series method. This enables the researchers to investigate the complete response of smart hybrid composite structures subjected to low velocity impact, the effect of shear deformation and the contact force independently. The effect and the role of some parameters such as the volume fraction, the orientation and the location of the SMA wires, the density of the impactor to the plate ratio (ρ_i / ρ_P),and the elastic modulus of the impactor to the plate ratio (E_i/E_{22P}) on impact response of smart hybrid composite plate is studied in details. Useful results to designers were obtained, which are not reported in similar literatures.

II. Basic Equations

Constitutive equations of principal stress-strain relationship for a SMA hybrid laminated composite are as presented by Zhong *et al.* [8], and Khalili *et al.* [12]:

F. Ashenai Ghasemi is the member of *Department of Mechanical Engineering, Shahid Rajaee Teacher Training University (SRTTU) Lavizan, Postal Code: 1678815811, Tehran, IRAN.* (corresponding author phone: Tel.: +98-21-22970052; fax: +1-678-8685363; E-mail: faramarz_ashenai_ghasemi@yahoo.com & f.a.ghasemi@srttu.edu).

A. Shokuhfar is the member of *Department of Mechanical Engineering, K. N. Toosi University of Technology Pardis Ave, Vanak SQ., Tehran, Iran.*

S. M. R. Khalili is the member of *Department of Mechanical Engineering, K. N. Toosi University of Technology Pardis Ave, Vanak SQ., Tehran, Iran.*

G. H. Payeganeh is the member of *Department of Mechanical Engineering, Shahid Rajaee Teacher Training University (SRTTU).*

K. Malekzadeh is the member of [3]*Department of Mechanical Engineering, Malek Ashtar University of Technology, Tehran, Iran.*

$$\begin{Bmatrix}\sigma_1\\ \sigma_2\\ \tau_{12}\end{Bmatrix}=\begin{bmatrix}Q_{11} & Q_{12} & 0\\ Q_{12} & Q_{22} & 0\\ 0 & 0 & Q_{66}\end{bmatrix}\begin{Bmatrix}\varepsilon_1\\ \varepsilon_2\\ \gamma_{12}\end{Bmatrix}+\begin{Bmatrix}\sigma_r\\ 0\\ 0\end{Bmatrix}k_s$$
$$-\begin{bmatrix}Q^m_{11} & Q^m_{12} & 0\\ Q^m_{12} & Q^m_{22} & 0\\ 0 & 0 & Q^m_{66}\end{bmatrix}\begin{Bmatrix}\alpha^c_l\\ \alpha^c_t\\ 0\end{Bmatrix}k_c\Delta T$$
$$\begin{Bmatrix}\tau_{13}\\ \tau_{23}\end{Bmatrix}=\begin{Bmatrix}Q_{55}\,0\\ 0 \quad Q_{44}\end{Bmatrix}\begin{Bmatrix}\gamma_{13}\\ \gamma_{23}\end{Bmatrix} \tag{1}$$

In the above equation, $\{\sigma\}$ represents the stresses in the principle directions. In addition, the matrix $\{\varepsilon\}$ represents the strains in the principle directions. Q_{ij} and Q^m_{ij} respectively represent the reduced stiffness matrices for the SMA hybrid composite and the composite medium (without the SMA wires). σ_r represents the recovery stress which can be determined analytically or by experiments (Birman *et al.* [7], Zhong *et al.* [8], and Rogers [9]). $\alpha^c{}_i$ ($i = l, t$) represents the thermal expansion coefficients of composite medium which is calculated based on the temperature difference ΔT between the current and the reference temperatures. k_s and k_c respectively represent the volume fractions of the SMA wires and the composite medium.

Because of discontinuity function of stresses through the thickness in each layer, it is possible to determine the constitutive equation by considering the force-couple resultants in terms of stresses, using integration of Equation (1) through the plate thickness, which yields:

$$\begin{Bmatrix}N\\ M\end{Bmatrix}=\begin{bmatrix}A_{ij} & B_{ij}\\ B_{ij} & D_{ij}\end{bmatrix}\begin{Bmatrix}\varepsilon^0\\ \kappa\end{Bmatrix}+\begin{Bmatrix}N^i\\ M^i\end{Bmatrix};\begin{Bmatrix}N^i\\ M^i\end{Bmatrix}=\begin{Bmatrix}N^r-N^T\\ M^r-M^T\end{Bmatrix}$$
$$;\ i,j=1,\ 2,\ 6$$
$$\{S\}=[k_{sh}A_{ij}]\{\gamma\};\quad i,j=4,5 \tag{2}$$

Where N and S are the vectors of forces and M is the vector of moments respectively. A_{ij}, B_{ij} and D_{ij} (i, j = 1, 2, 6) are the matrices of extensional, coupling and bending stiffness respectively. N^r and M^r respectively represent the vectors of recovery stress resultants and stress moments generated in the SMA wires. N^T and M^T respectively represent the vectors of the thermal stress resultants and moments in the structure. Also ε^0 and γ are the midplane and shear strains and κ is the curvature respectively. In symmetrically laminated cross-ply plates: $B=M^i=M^r=M^T=0$.

The plate equations developed by Whitney *et al.* [13] are used as they included the effect of transverse shear deformations. Reducing those equations to specially orthotropic form (B_{ij} = 0, $A_{16} = A_{26} = D_{16} = D_{26} = 0$), and adding the uniform in-plane initial stress resultants N^i_x and N^i_y as discussed by Sun *et al.* [14] results in:

$$D_{11}\,\psi_{x,xx}+D_{66}\,\psi_{x,yy}+(D_{12}+D_{66})\psi_{y,xy}$$
$$-k_{sh}\,A_{55}\,\psi_x-k_{sh}\,A_{55}\,w_{,x}=I\ddot{\psi}_x$$
$$(D_{12}+D_{66})\,\psi_{x,xy}+D_{66}\,\psi_{y,xx}+D_{22}\,\psi_{y,yy}$$
$$-k_{sh}\,A_{44}\,\psi_y-k_{sh}\,A_{44}\,w_{,y}=I\ddot{\psi}_y$$
$$k_{sh}\,A_{55}\,\psi_{x,x}+(k_{sh}\,A_{55}+N^i_x)\,w_{,xx}$$
$$+k_{sh}\,A_{44}\,\psi_{y,y}+(k_{sh}\,A_{44}+N^i_y)\,w_{,yy}+q=\rho\ddot{w} \tag{3}$$

k_{sh} is the shear correction factor introduced by Mindlin [15], normally taken to be $\pi^2/12$. In addition, q is the dynamic normal load (transverse impact) over the plate and:

$$(A_{ij},B_{ij},D_{ij})=\int_{-h/2}^{h/2}\overline{Q}^k_{ij}(1,z,z^2)\,dz$$
$$(\rho,I)=\int_{-h/2}^{h/2}\rho_0\left(1,z^2\right)dz \tag{4}$$

In the above relation, ρ_0 represents the density of each layer and ρ is the total density of the plate. In addition, I is the moment of inertia and h is the thickness of the plate. $(\overline{Q}_{ij})_k(i,j=1,2,6)$ and $(\overline{Q}_{ij})_k(i,j=4,5)$ are the transformed reduced stiffness of each layer that are defined in Sun *et al.* [14].

In this work, attention is focused upon a simply supported rectangular plate with the dimensions of a and b. Hence, the boundary conditions are as follows:

$$w=\psi_{x,x}=\psi_y=0\quad ;\quad at\ \ x=0,a$$
$$w=\psi_{y,y}=\psi_x=0\quad ;\quad at\ \ y=0,b \tag{5}$$

Fig. 1 shows a smart composite structure, which is in contact with an impactor mass.

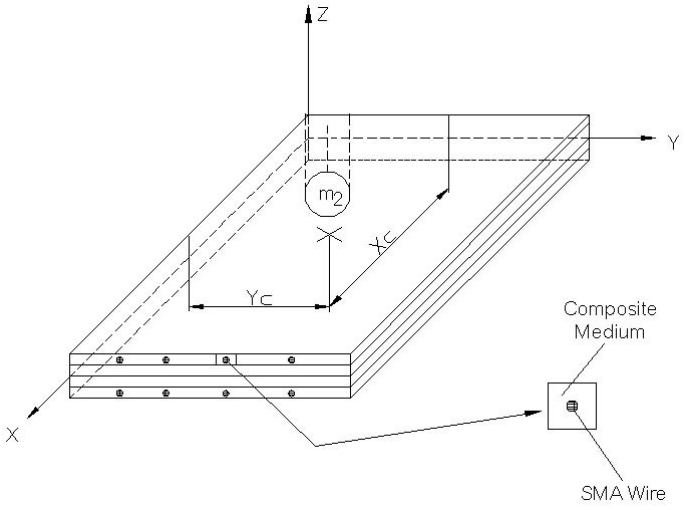

Fig. 1 Schematic view of smart composite structure impacted by a spherical mass.

III. DYNAMIC RESPONSE OF THE PLATE

In the present analysis, two degrees of freedom springs-masses model (Abrate [3], Khalili *et al.* [16]) is utilized to determine the contact force of the impact (Fig. 2). The equation of motion is as follows (Abrate [3]):

$$m_2 \ddot{z}_2 + F = 0 \qquad (6)$$

$$m_1 \ddot{z}_1 + K_{bs} z_2 + K_m z_2^{\,3} - F = 0$$

Where F is the contact force, m_1 and m_2 represents respectively the mass of the hybrid plate and the impactor, z_1 and z_2 are respectively the relative displacements of the hybrid plate and the impactor masses. $K_l = K_{bs}$ is the bending-shear stiffness, K_b is the bending stiffness, K_s is the shear stiffness, and K_m is the membrane stiffness of the hybrid plate. Since the membrane stiffness K_m is low in polymer composite materials especially in low velocities and low deflections, ignoring this parameter from the current model in Fig. 2(a) would result in changing the model into a simplified one illustrated in Fig. 2(b). Hence, using Choi's linearized model (Choi *et al.* [17]) instead of nonlinear Hertzian contact law, the contact force can be obtained as (Khalili *et al.* [12]):

$$F(t) = K_l . \alpha = K_l . (z_2 - z_1)$$

$$K_l = F_m^{\,1/3} . K_c^{\,2/3} \qquad (7)$$

In the above equations, $K_2 = K_l$ represents the linearized contact coefficient in Choi's linearized contact law, F_m is the maximum predicted contact force, and K_c represents the contact stiffness in the improved Hertzian contact law, which can be calculated based on the following equation (Choi *et al.* [17]):

$$K_c = \frac{4}{3} \frac{R^{1/2}}{\frac{1-\upsilon^2}{E} + \frac{1}{E_{22}}} \qquad (8)$$

Where R is the curvature radius, ν is the Poisson's ratio and E is the elastic modulus of the isotropic impactor. Because the plate is not isotropic, it must be mentioned that the parameter E_{22} is the transverse elastic modulus of the top lamina of the structure.

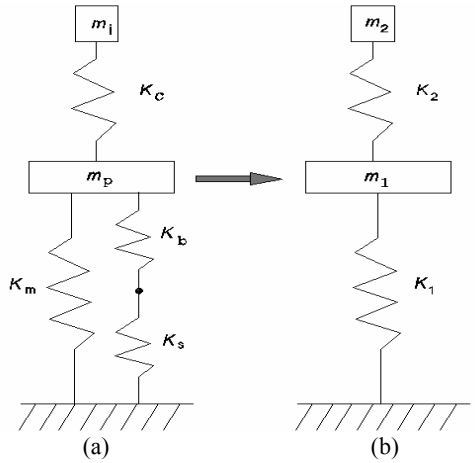

Fig. 2 A two-degrees of freedom springs-masses model: (a) with the membrane stiffness and (b) without the membrane stiffness (Abrate *et al.* [3], and Khalili *et al.* [12]).

Considering the free body diagram in Fig. 2(b) and replacing the value of F in Equation (6) with the value presented by Choi's differential equations after rearrangements, it can be converted to the following form Khalili *et al.* [12]:

$$m_1 \ddot{z}_1 = -K_1 z_1 - K_2 (z_1 - z_2) \qquad (9)$$

$$m_2 \ddot{z}_2 = -K_2 (z_2 - z_1)$$

This system can be solved easily by Runge-Kutta method using ODE solver of the MATLAB software.

The solution to the dynamic problem is based on expansions of the loads, displacement, and rotations in double Fourier series. Each expression is assumed to be separately consisting of a function of position and a function of time. Furthermore, by neglecting the effects of rotary inertia (Bert *et al.* [18]), the current problem could be converted to a system of ordinary differential equations of second-order in time for the Fourier coefficients of the transverse deflection (Birman *et al.* [7]). The contact force obtained by the present procedure (See Equation (7)) is used as an input for further analysis of the hybrid composite plate, like the deflection under the point of impact and the failure prediction of the plate, etc. The load function can be demonstrated as follows (Carvalho *et al.* [19]):

$$q(x,y,t) = \sum_m \sum_n P_{mn}(t) . Sin\ (\frac{m\pi}{a})x . Sin\ (\frac{n\pi}{b})y \qquad (10)$$

Where $P_{mn}(t)$ are the terms of the Fourier series. For a concentrated load located at the point (x_c, y_c):

$$P_{mn}(t) = \frac{4F(t)}{ab} . Sin\ (\frac{m\pi}{a})x_c . Sin\ (\frac{n\pi}{b})y_c \qquad (11)$$

Where $F(t)$ is the impact load (See Equation (7)) and a and b are respectively the plate length and width.

The impact solution for a rectangular plate with simply supported boundary conditions is assumed to be in the following form (Carvalho *et al.* [19]):

$$\psi_x(x,y,t) = \sum_{m,n=1}^{\infty} A_{mn}(t) . Cos\ (\frac{m\pi}{a})x\ . Sin\ (\frac{n\pi}{b})y$$

$$\psi_y(x,y,t) = \sum_{m,n=1}^{\infty} B_{mn}(t) . Sin\ (\frac{m\pi}{a})x\ . Cos\ (\frac{n\pi}{b})y$$

$$w(x,y,t) = \sum_{m,n=1}^{\infty} W_{mn}(t) . Sin\ (\frac{m\pi}{a})x\ . Sin\ (\frac{n\pi}{b})y \qquad (12)$$

Where $A_{mn}(t)$, $B_{mn}(t)$ and $W_{mn}(t)$ are the time dependent coefficients.

As mentioned earlier, by neglecting the rotary inertia effect (Mindlin [15]) and using the Equation (12), the system of Equations (3) can be reduced to an ordinary decouple differential equations, then following procedure of Christoforou *et al.* [20] and using the changes of variables, the governing equations of the plate can be simplified as follows:

$$\ddot{W}_{mn}(t) + \omega_{mn}^2 W_{mn}(t) = \frac{P_{mn}(t)}{\rho h} \qquad (13)$$

ω_{mn}^2 is the square of the fundamental frequencies of the plate. If the value of $m = n = 1$ is inserted in the above expression, the value of K_{bs} in Equations (6) could be calculated as follows:

$$K_{bs} = m_1 . \omega_{11}^2 \qquad (14)$$

For zero initial displacement and velocity, the solution of Equation (13), namely the value of $W_{mn}(t)$, would be easily calculated based on the Runge-Kutta method of 4th and 5th ranks and using a software like MATLAB and its ODE 45 solver. Substituting these values in Equation (12), the values of w, ψ_x and ψ_y would be easily calculated.

If the above quantities are determined, then the values of strains will be easily calculated (Reddy [21], and Khalili *et al.* [22]).

IV. VERIFICATION OF THE MODEL

To ensure the accuracy of the present model, the contact force determined from the springs-masses model is compared with the contact-force determined from Choi's dynamic model Choi *et al.* [17]. Fig. 3 shows a good agreement in the results. The effect of increasing the number of terms of the Fourier series included in the solution for the transverse deflection of the plate is illustrated in Fig. 4. Fig. 4 shows that a reasonable solution is obtained using as much as 9 terms, but the convergence is demonstrated with 100 terms.

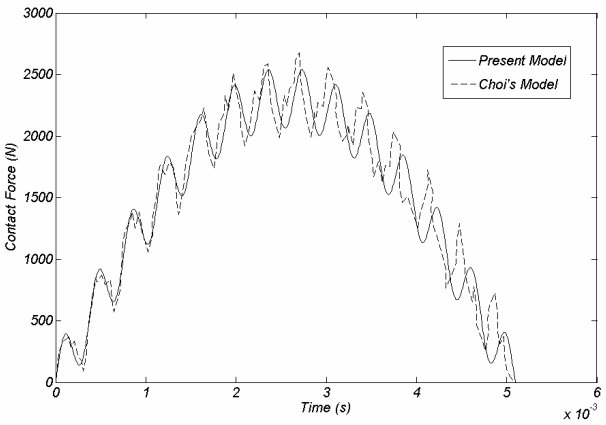

Fig. 3. Comparison of the contact force from the present model and Choi's model [17].

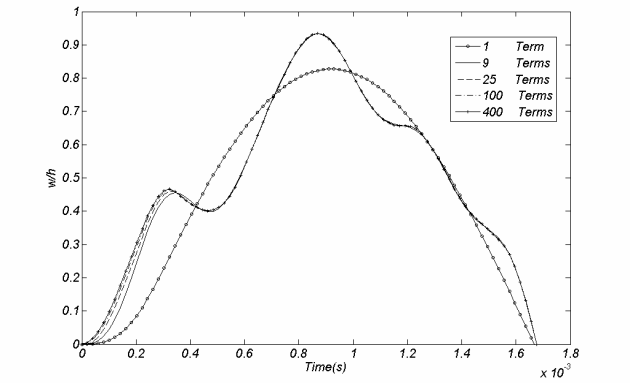

Fig. 4. Effect of varying the number of terms in Fourier series on transverse deflection of the plate.

V. RESULTS AND DISCUSSION

The hybrid composite plate used is symmetric and cross ply. The impactor is a spherical object. Geometrical and material properties of the composite plate as well as the impactor are presented in Table. 1 (Birman *et al.* [7]; Reddy [21]). The laminate consists of 10 layers and they are numbered from top to bottom. In this research, the SMA wires embedded only parallel to the fibers of the composite medium. If the orientations of the SMA wires do not be in the same direction of composite medium fibers, the mismatching of fibers and the SMA wires causes some non-fiber spaces in which contain only brittle resin. This phenomenon causes brittle fracture and results in the reduction of structure properties (Tsoi *et al.* [23]). The volume fractions of the SMA wires are considered to be k_{sx} = 0.05, 0.10 and 0.15. The wires were placed only along the *x*-direction, which corresponds to the 0° fiber orientation in composite medium and only in the layers 5 and 6.

Table. 1. Geometrical and material properties of the hybrid composite plate and impactor (Birman and Chandrashekhara, 1996; Reddy, 2004).

Geometrical properties of SMA hybrid composite	
Boundary conditions	Simply supported
Length = Width	200 mm
Lay-up	$[0/90/0/90/0]_s$
Ply thickness	0.269 mm
Properties of composite medium (Graphite-Epoxy)	
E_{11} = 141.2 GPa ; $E_{22} = E_{33}$ = 9.72 GPa	
$G_{13} = G_{12}$ = 5.53 GPa ; G_{23} =3.74 GPa	
$v_{12} = v_{13} = v_{23}$ = 0.30	
ρ = 1536 kg/m^3	
Properties of the SMA wires (Ni-Ti based in austenite form)	
E = 70 Gpa, G = 26.32 GPa, v = 0.33 ρ = 6500 kg/m^3, σ_r = 220 MPa at ΔT = 39 °C	
Properties of impactor	
E = 207 GPa, v = 0.3, ρ = 7800 kg/m^3	
Tip diameter =12.7 mm	
Weight = 2.5 _ (Plate weight)	
Velocity = 2.50 m/s	

Fig. 5(a) shows the maximum value of *w/h* ratio (a non-dimensional transverse deflection, which is the ratio of composite plate deflection to its thickness) decreases from 0.9308 in the composite medium (the composite without SMA wires, or k_{sx} = 0.00, curve 1) to 0.4931 in the smart hybrid composite in which the SMA wires have the volume fraction of 0.15 (curve 4). Thus, 47 percent reduction is occurred. As it is evident in Fig. 5(b), by increasing the volume fraction of SMA wires, the maximum contact force (hereinafter-called MCF) increases from 901.6 N in the case of composite without SMA wires to 1129 N in the case that the volume fraction of the SMA wires is equal to 0.15. The MCF was increased by 25 percent, while the maximum contact force

time (MCFT) tends to move to the right side of the diagram by the distance d in Fig. 5(b), and the contact time (CT) was increased from 347.2 μs to 423.8 μs. Thus, the shocking effect of the impact force transfers to the plate decreases and a weaker impact inflicted upon the structure.

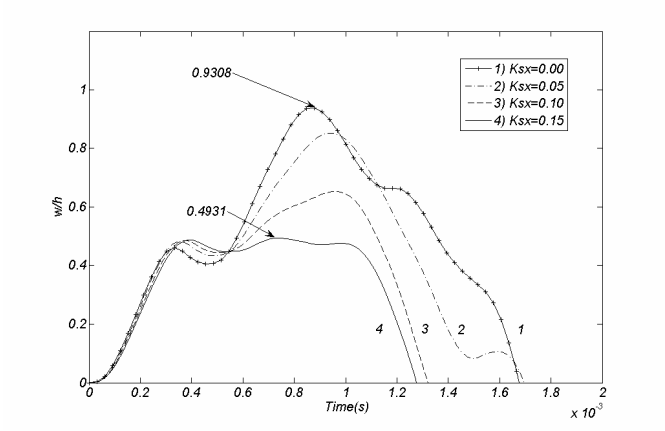

(a)

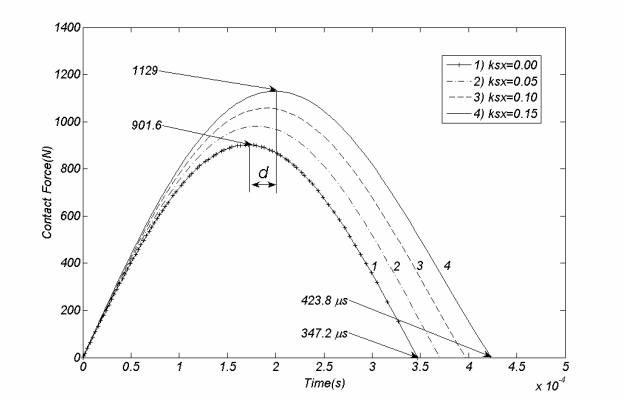

(b)

Fig. 5 (a) Effect of increasing the volume fraction of the SMA wires on non-dimensional deflection (w/h) history and (b) Effect of increasing the volume fraction of the SMA wires on contact force history.

Therefore reducing the damage imparted to the structure, increasing the damage tolerance properties. Here is an interesting difference between the pre-stressed laminated hybrid composite plate and the pre-stressed composite plate without the SMA wires, as the author reported earlier (Khalili *et al.* [24]). They presented that the initial tensile stresses on a laminated composite plate without the SMA wires would increase the MCF and the MCFT, but decrease the CT. This would decrease the deflection of the structure, but increase the shock nature of the impact, where as in the case of hybrid composite the pre-stressed nature of the SMA wires would increase the CT and hence reduces the impact shock of the plate. Therefore, it seems that the pre-stressed laminated composite structures with the SMA wires have more beneficial effect than traditional pre-stressed laminated composite plates.

The in-plane strains and stresses during the time which the impactor hits the structure and then separates from the structure are also important. Fig. 6 demonstrates the variation of the in-plane strains and stresses with time, when the volume fraction of the SMA wires increases parallel to the x-axis in layers 5 and 6.

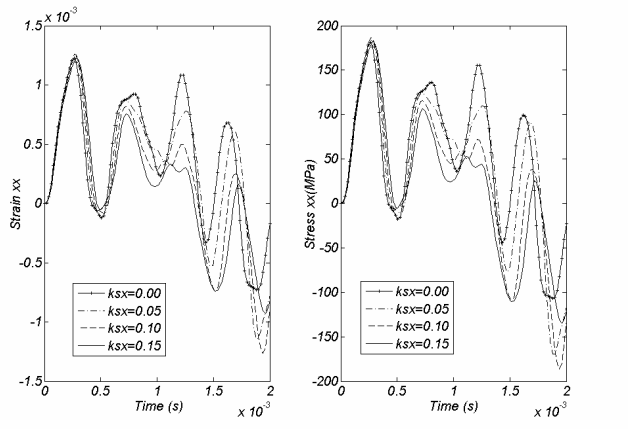

(a) (b)

Fig. 6 (a) Variation of strain xx with time; (b) Variation of stress xx with time.

Comparison of the Fig. 5(b) and Fig. 6 together is interesting. As it is evident in Fig. 5(b), the CT is about 400 μs for all the cases studied. This is the time when the impactor separates from the structure. By observing the curves in Fig. 6 more carefully, one may notice that the effect of SMA wires upon the in-plane strains and stresses before the separation of the impactor and the plate is very small. The maximum values of strains and stresses are reduced less effectively and they tend to move to the right side of the diagrams as the volume fraction of the SMA wires increases. Therefore, their behavior resembles the MCF behavior demonstrated in Fig. 5(b) as the volume fraction of the SMA wires increases.

The important point is that at the end of the CT, the difference of strains and stresses increases drastically. The main effect of the SMA wires that reduces the in-plane strains and stresses becomes apparent when the transverse loading is ended. This is because the impact force inflicted in a very short period. Since the impact wave velocity is less compared to the impact period, the composite plate with the SMA wires will respond with a delay. The occurrence of the maximum point of the in-plane strains and stresses was shown in Fig. 7. The plate with the SMA wires will damp more uniformly and rapidly than the plate without the SMA wires after the CT.

The occurrence of the maximum point of the in-plane strains and stresses was shown in Fig. 7. The plate with the SMA wires will damp more uniformly and rapidly than the plate without the SMA wires after the CT.

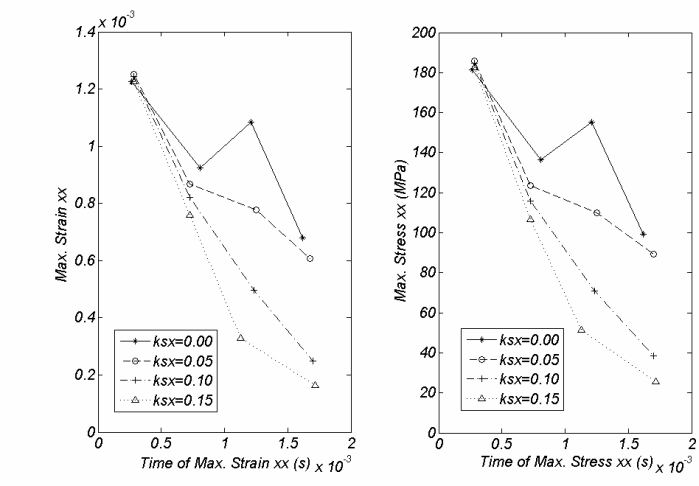

(a) (b)

Fig. 7 Effect of volume fraction of the SMA wires on: (a) maximum strain *xx*, (b) maximum stress *xx*.

Here the effect of through thickness location of the SMA wires inside the composite structure. Since the SMA wires with volume fraction of 0.15, reinforced the structure resistance more effectively, at this stage the volume fraction is chosen 0.15. The SMA wires are embedded along the *x*-axis.

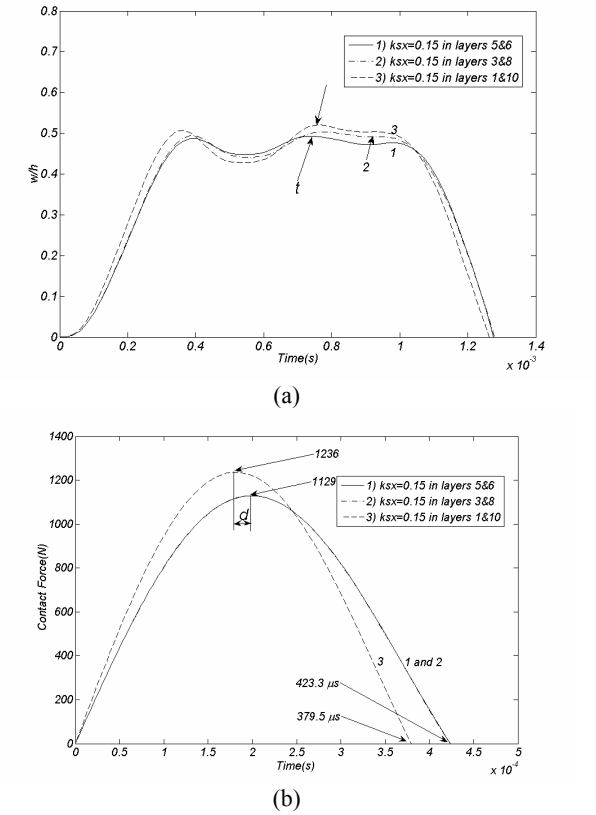

(a)

(b)

Fig. 8 Effect of through thickness location of the SMA wires on: (a) *w/h* ratio and (b) contact force history.

Figs. 8(a) and 8(b) show this effect. Fig. 8(b) shows that when the SMA wires embedded along the *x*-direction within the layers 5 and 6 (i.e. near the mid-plane of the structure) and also in the layers 3 and 8, no changes would occur in the MCF (1129 N, curve 1 and 2). If the through thickness location of the SMA wires is changed from the previous positions into the upper and the bottom surfaces (layers 1 and 10), it would increase the MCF, but decreases the MCFT and the CT (curve 3). This happens, since the impact is a local phenomenon. For the above example, in which the composite medium was considered to be graphite-epoxy, if the SMA wires embedded in the top layer, the impactor hits a stiffer layer and so the MCF increases but the MCFT and the CT decrease. Therefore, the impact produces a greater shock and the structure experiences the largest impact load (in comparison with the plate having the SMA wires at the middle). The increased discrepancy *t* between the curves of *w/h* that is shown in Fig. 8 (a) also confirms this. Therefore by placing the SMA wires far from the mid-plane and on the top and bottom layers of the composite plate, not only increases the local impact resistance, but also increases the global deflection of the structure.

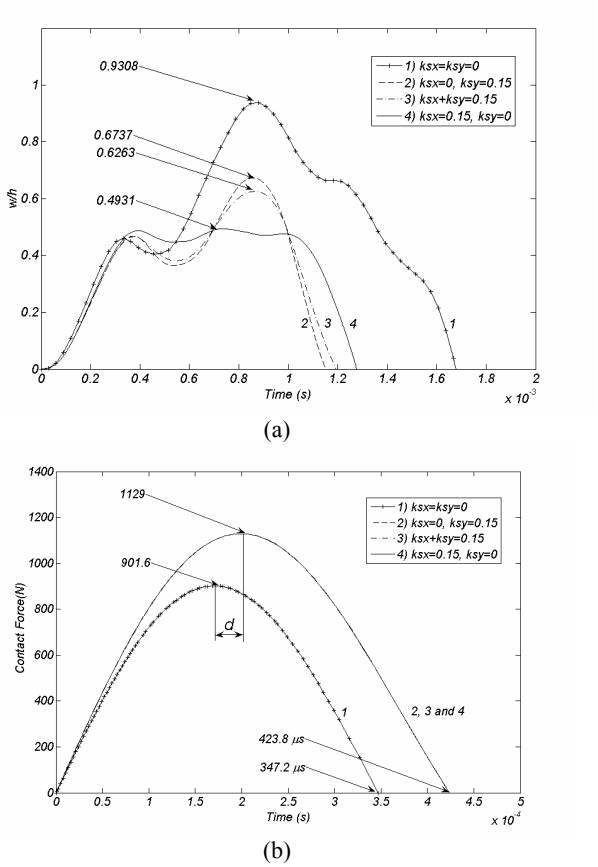

(a)

(b)

Fig. 9 Effect of orientation of the SMA wires on: (a) *w/h* ratio and (b) contact force history.

It was mentioned earlier that the impact resistance of graphite/epoxy composites could be improved by increasing the volume fraction of the SMA wires or by embedding the SMA wires in the middle layers of the structure. The SMA wires can be embedded in their fixed location within the

middle layers of the structure as: 1) in the layers 5 and 6 along the *x*-direction, 2) in the layers 4 and 7 along the *y*-direction and 3) simultaneously in the layers 5, 6, and 4, 7 in both the *x* and *y* directions respectively with the fixed volume fraction equal to 0.15 (curves 2, 3 and 4 in Fig. 9 (a)). These cases were studied compared with the case of composite plate without the SMA wires (curve 1 in Fig. 9 (a)). Figs. 9 (a) and (b) show the transverse deflection and the contact force histories of the above cases. The results indicated that because the SMA wires improve the impact resistance of the composite structure (the MCF increases, but the MCFT moves to the right side of Fig. 9(b)), hence the shock effect of the impact force decreases. Changing the wire orientation, does not affect the amount of the contact force. Fig. 9 (a) demonstrates that the reduction of the maximum value of *w/h* of the curve 4 is 47% smaller than the curve 1 (value of 0.4931 compare to 0.9308). It shows that the orientation of the SMA wires has a greater effect in curve 4 as compared to the other cases. A similar behavior was observed in the amount of the in-plane strains and stresses, which are not shown here.

The deflection-contact force diagram of the whole structure is shown in Fig. 10 in order to study the dynamic behavior of the structure. The areas below the curves indicate the amount of energy dissipation in the structure. As it can be observed, comparing the curves 1 and 4 indicates that the energy dissipation increases by % 56. The above increase is % 51 in the case of curve 2 and % 49 in the case of curve 3. Hence, it shows that the orientation of the SMA wires has a greater effect in the curve 4 as compared to the others. The energy dissipation of the plates with embedded the SMA wires cause the increase of impact resistance and the damage tolerance of the structure and hence decreases its brittle behavior as well as decreases the deflection, the in-plane strains, and stresses. Hence, it protects the structure against impact.

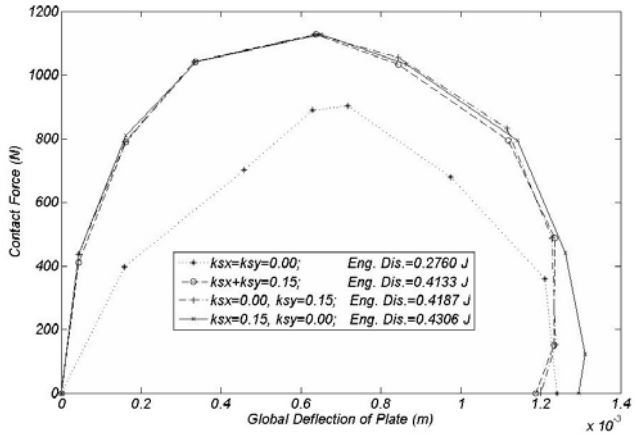

Fig. 10 The contact force in terms of global deflection of structure with regard of orientation of the SMA wires.

The effect of various density of the impactor (ρ_i) to the plate (ρ_P) ratio (which in accordance to the Table. 1 is equal to ρ_i / ρ_P = 3.5) is examined here. The volume fraction of SMA wires is constant and equal to 0.15. Their through thickness location are in the middle of the structure (here, layers 5 and 6) and they are only embedded in *x* direction. To study the effect of ρ_i / ρ_P ratio, three ratios 1, 3.5 and 10 are considered.

The effect of this change is shown in Fig. 11. As it is visible, this parameter has no effect on the impact force and *w/h* ratio of the structure. This also means that SMA wires have their positive effect on the impact behavior of the composite structures with a large range of densities of the impactor, which collide to them.

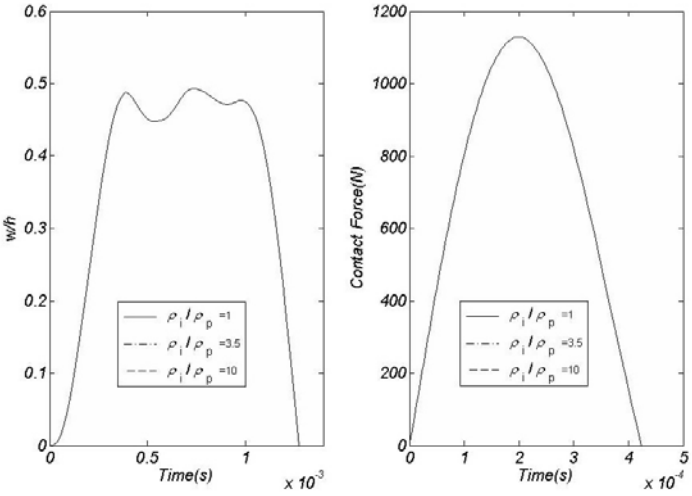

(a) (b)

Fig. 11 Effect of ρ_i / ρ_P ratio on: (a) *w/h* ratio and (b) contact force history.

The effect of various elastic modulus ratio of the impactor (E_i) to the transverse plate modulus (E_{22P}) (which in accordance with Table. 1 is equal to E_i/E_{22P} = 21) is examined here. The volume fraction of SMA wires is constant and equal to 0.15. The through thickness location are in the middle of the structure (here, layers 5 and 6) and they are only embedded in *x* direction. To study the effect of E_i/E_{22P} ratio, three ratios 21, 40 and then 100 are considered namely.

The effect of changes in modulus ratio is shown in Fig. 12. Fig. 12(a) shows that the maximum value of *w/h* ratio of the structure increases, which is not desirable either. Fig. 12(b) shows that if this parameter increases from 21 to 100, the impact response of the structure is shortly amplified. This is because that MCF increases but MCFT and CT decrease. These phenomena increase the impact shock that simplify the damage of the structure.

The reason of these phenomena is that by increasing the above elastic modulus ratios, in fact a stiffer subject affect the plate. Hence, the impact shock and maximum *w/h* ratio increase. However, it must be noted that by increasing the above ratios (E_i/E_{22P} from 21 to 100), *w/h* ratio, and impact force parameters increase only about 1 percent. This also means that SMA wires have their positive effect on the impact behavior of the composite structures with a large range of densities of the impactor, which collide to them.

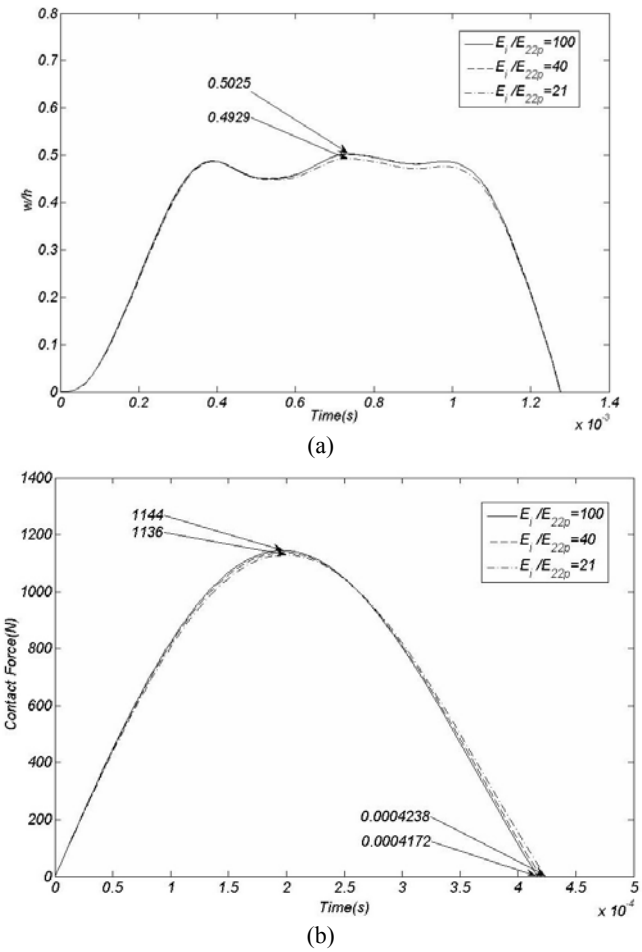

Fig. 12 Effect of E_i/E_{22p} ratio on: (a) *w/h* ratio and (b) contact force history.

VI. CONCLUSIONS

In this paper, a complete model is developed to study the response of low velocity impact upon the smart hybrid composite structures. The following conclusions are obtained:

1- The use of SMA wires inside the unidirectional hybrid composite plates improve the global behavior of the structure against the impact. The plate with the SMA wires damp more uniformly and rapidly than the plate without the SMA wires after the impact.

2- The volume fraction of the SMA wires could affect the MCF, the MCFT and the CT. Hence, the shocking effect of the impact imparted to the plate can be changed accordingly. These changes occur in the deflection and the in-plane strains and stresses.

3- The location of the SMA wires can change the overall and the local behavior of the structures. Placing the SMA wires on the top and bottom layers in the laminate could improve the local behavior, while placing the wires in the mid-plane could affect the overall behavior of the structures. Placing the SMA wires in the composite medium also could affect better in energy dissipation of the structures and hence improve the damage tolerance.

4- If the orientations of the SMA wires were along the orientation of the majority of fiber in the composite medium laminate, it would more effect and improve the global behavior of the structure.

5- The SMA wires can improve the impact resistance of the composite structures, in different value of density ratio of the impactor to the plate and in different value of the elastic modulus ratio of the impactor to the transverse elastic modulus of the plate too.

REFERENCES

[1] S. Anca, C. Diana, M. Baritz, and F. Margareta, "Simulation of Mechanical Properties for Fibre Reinforced Composite Materials," *Proceedings of the 3rd IASME / WSEAS International Conference on CONTINUUM MECHANICS (CM'08) 2008*, Cambridge, UK, pp. 146-149.

[2] H. Teodorescu, S. Vlase, D. Nicoara, V. Guiman, "Mechanical behaviour of pre-tensioned glass fiber reinforced composite tubes subjected to internal pressure," *Proceedings of the 2nd IASME / WSEAS International Conference on Continuum Mechanics (CM'07) 2007*, Portoroz, Slovenia, pp. 84-89.

[3] S. Abrate, "Modeling of impacts on composite structures," *Composite Structures*, vol. 51, pp. 129-138, 2001.

[4] R. Olsson, "Analytical prediction of large mass impact damage in composite laminates," *Composites: Part A*, vol. 32, 2001, pp. 1207-15.

[5] R. Olsson, "Closed form prediction of peak load and delamination onset under small mass impact," *Composite Structures*, vol. 59, 2003, pp. 341-349.

[6] C. T. Sun, J. K. and Chen, "On the impact of initially stressed composite laminates," *Journal of Composite Materials*, vol. 19, 1985, pp. 490-503.

[7] V. Birman, K. Chandrashekhara, and S. Sain, "An approach to optimization of shape memory alloy hybrid composite plates subjected to low-velocity impact," *Composites: Part B*, vol. 27B, 1996, pp. 439-446.

[8] Z. W. Zhong, R. R. Chen, C. Mei, and C. S. Pates,. "Buckling and post-buckling of shape memory alloy fiber reinforced composite plates," In: "*Buckling and Postbuckling of Composite Structures*," Ed. A. K. Noor, ASME, New York, 1994, pp. 115-132.

[9] C. A. Rogers, "Active vibration and structural acoustic control of shape memory alloy hybrid composites: experimental results," *Journal of Acoustics Society of America*, vol. 88, 1990, pp. 2803-2811.

[10] L. McD. Schetky, "The role of shape memory alloys in smart/adaptive structures." In: "*Shape memory Materials and Phenomena-Fundamental Aspects and Applications*," Eds C. T. Liu, Materials Resource Society, Pittsburgh, 1992, pp. 299-307.

[11] J. H. Roh, and J. H. Kim, "Adaptability of Hybrid smart composite plate under low velocity impact," *Composites: Part B*, vol. 34, 2003, pp.117-125.

[12] F. Ashenai Ghasemi, A. Shokuhfar, G. H. Payeganeh, and K. Malekzadeh, "Modeling and simulation of the dynamic response of smart hybrid composite structures subjected to low-velocity impact," *11th WSEAS Int. Conf. on Automatic Control, Modeling and Simulation 2009*, Istanbul, Turkey, Paper code: 614-163.

[13] J. M. Whitney, and N. J. Pagano, "Shear deformation in heterogeneous anisotropic plates," *Journal of Applied Mechanics*, vol. 37, 1970, pp. 1031-1036.
[14] C. T. Sun, and S. Chattopadhyay, "Dynamic Response of Anisotropic Plates Under Initial Stress Due to Impact of a Mass," Transactions of the ASME, *Journal of Applied Mechanics*, vol. 42, 1975, pp. 693-698.
[15] R. D. Mindlin, "Influence of rotary inertia and shear on flexural motions of isotropic elastic plates," *Journal of Applied Mechanics*, vol. 18, 1951, pp. 31-38.
[16] M. R. Khalili, K. Malekzadeh, and R. K. Mittal, "Effect of physical and geometrical parameters on transverse low-velocity impact response of sandwich panels with a transversely flexible core," *Composite Structures*, vol. 77, 2007, pp. 430-443.
[17] I. H. Choi, and C. H. Lim,. "Low-velocity impact analysis of composite laminates using linearized contact law," *Composite Structures*, vol. 66, 2004, pp. 125-132.
[18] C. W. Bert, and V. Birman, "Dynamic stability of thick, orthotropic, circular cylindrical shells," In: "*Lecture Notes in Engineering: Refined Dynamic Theories of Beams, Plates and Shells and Their Applications,*" Eds by I. Elishakoff and H. Irretier, Springer, Berlin, 1987, pp. 235-244.
[19] A. Carvalho, and C. G. Soares, "Dynamic response of rectangular plates of composite materials subjected to impact loads," *Composite Structures*, vol. 34, 1996, pp. 55-63.
[20] A. P. Christoforou, and S. R. Swanson, "Analysis of Impact response in composite plates," *International Journal of Solids Structures*, vol. 27(2), 1991, pp. 161-170.
[21] J. N. Reddy, "Introduction to composite materials," *Mechanics of laminated composite plates and shells*, Second Edition, United States of America: 88, CRC Press, 1997.
[22] M. R. Khalili, K. Malekzadeh, and R. K. Mittal, "A new approach to static and dynamic analysis of composite plates with different boundary conditions," *Composite Structures*, vol. 69, 2005, pp. 149-155.
[23] K. A. Tsoi, R. Stalmans, J. Schrooten, and Y. W. Mai, "Impact damage behavior of shape memory alloy composites," *Materials Science and Engineering Part: A*, vol. 342, 2003, pp. 207-215.
[24] S. M. R. Khalili, R. K. Mittal, and N. Mohammad Panah, "Analysis of fiber reinforced composite plates subjected to transverse impact in the presence of initial stresses," *Composite Structures*, vol. **77,** 2006, pp. 263-268.
[1]